FABRICATION AND MULTIFUNCTIONAL CHARACTERIZATION OF HYBRID WOVEN COMPOSITES REINFORCED BY ALIGNED CARBON NANOTUBES

Namiko Yamamoto*, Enrique J. Garcia*, A. John Hart*, Brian L. Wardle*, Alexander H. Slocum*
***Massachusetts Institute of Technology, Cambridge, MA, USA**

Keywords: *CNT, Multi-functional Properties, intralaminar, epoxy, electrical, resistivity, conductance, damping, VACNT*

Abstract

Hybrid composite architectures employing traditional advanced composites and aligned carbon nanotubes (CNTs) offer significant multifunctional performance benefits in addition to enhanced structural properties. This broadens potential applications of these hybrid composites, e.g., with improved electrical conductivity, the composites may have application in lightning-strike protection. Our previous work has explored fabrication of such composites, including aligned CNT growth on filaments/tows/weaves, wetting with a polymeric matrix, and mechanical testing of the hybrid composites. Along with fabrication advances, this paper focuses on multifunctional properties of a composite consisting of woven alumina ceramic filaments, CNTs, and a thermoset matrix. Properties explored include through-thickness and in-plane electrical conductivities, and damping of baseline and CNT-enhanced hybrid composites. Excellent wetting and low void fractions are demonstrated by optical and scanning electron microscopy inspection of laminate cross-sections. Electrical resistivities decrease significantly ($x10^{-6}$-10^{-8}) with increasing CNT volume fraction. Damping ratio is not significantly affected by CNT volume fraction, suggesting strong bonding between the (unfunctionalized) CNTs and the matrix. Further improvements in manufacturing of the hybrid composite specimens, and investigations of other multifunctional properties (e.g., thermal conductivity and thermal expansion) will be pursued as future work.

1 Introduction

Since Iijima confirmed their cylindrical-wall structure in 1991 [1], carbon nanotubes (CNTs) have been rigorously investigated for their exceptional properties. For example, CNTs have high tensile stiffness (~1 TPa, [2-5]) and strength, and these density-normalized values exceed all other natural and synthetic materials. Their individual electrical conductivities vary from semiconducting to metallic depending on the tube diameter and wrapping angle (chirality) [6-8], which determines their band gap [9-10]. In addition, thermal conductivity of CNTs is theoretically estimated to be high for graphene sheets in tube configuration [9, 11], and thermal conductivity of SWCNTs was experimentally measured as 3500 W/m-K [12]. CNTs and CNT composites are also expected to have high damping due to their nano-scale size, low density, and therefore a large surface area to mass ratio [13-14]. Individual CNTs and groups of CNTs have been employed as micro-probes and data storage elements due to their mechanical resilience [15-16] and high electrical conductance [18-20]. Meanwhile, there is parallel interest in integration of CNTs in macro-scale structures, especially in aeronautical or space structures that require light weight and stability in extreme thermal/radiation environments. However, the maximum length of continuous CNTs is currently limited to ~10 mm [21-25], and therefore in order to take advantage of the outstanding properties of the CNTs, advanced

composite architectures must integrate CNTs at much larger scales [26].

The most direct structural application of CNTs is by their integration into existing composite materials to form hybrid architectures. Various CNT reinforcements in polymer matrices have been investigated [5, 11, 26-30]. Mechanical property improvements of the polymers were observed, but were typically moderate due to poorly dispersed and highly entangled CNTs with very limited volume fraction (typically <2 %), and/or low interfacial (CNT-matrix bond) strength [26-27]. To improve the dispersion of CNTs, unlike the composite examples given above made of CNTs dispersed solely in epoxy, composites used in this work are made of micron diameter filaments with CNTs grown on their surfaces [31], as shown in Fig.1 [32-33]. The mechanical properties of these hybrid composites exhibit significant improvements over the non-CNT architecture [33], and electrical, thermal, and damping properties due to CNTs are also expected to be improved.

Such a hybrid composite design has three major advantages. First, direct growth on advanced filaments allows uniform dispersion of aligned CNTs in the composites. Randomly oriented dispersed CNTs often form agglomerates [30, 34] limiting good CNT dispersion. When some techniques (sonication [30], or calandering [34]) are used to avoid this agglomeration, the volume fraction of CNT in the polymer matrix between filaments is very small (0.12 wt% [34]) due to the high viscosity of the CNT/polymer blend that must impregnate the filaments. With aligned CNTs grown on filaments as in this work, high weight fractions and excellent dispersion is expected, allowing the benefits of the CNTs to be incorporated in the hybrid composites in a highly-ordered way. Second, aligned CNTs on adjacent filaments overlap with one another in the stacked layer structure as shown in Fig.1. The CNTs bridge the ply interlayer in addition to everywhere in the matrix (and therefore the laminate) [32-33], and provides conductive pathways/percolation. Third, the thermal chemical vapor deposition (CVD) method employed in this work allows very rapid growth (> 2 μm/sec) of high-quality aligned CNTs (~7 nm in diameter) at atmospheric pressure [35-36].

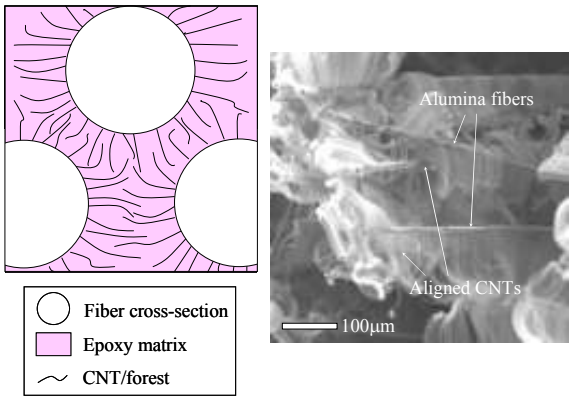

Figure 1. Cross-sectional schematic of the hybrid composites (left, not to scale), and SEM picture of ~100μm CNTs grown on the surface of alumina fibers.

In this work, hybrid epoxy-matrix composites consisting of aligned CNTs, woven alumina filament cloth, and epoxy were evaluated for wetting and for their improvement in electrical resistivity, damping ratio, and Young's modulus, relative to laminated alumina filament cloths without CNTs. A similar hybrid composite architecture involving CNTs grown with a different process on Silicon Carbide (SiC) cloth has reported large improvements in both mechanical and multi-functional properties [37].

2 Sample Fabrication

In the following section, an overview of the CNT growth and composite fabrication is provided, along with the morphology of the composite samples.

2.1 Growth of CNTs

Alumina (Al_2O_3) filament cloth was selected as the substrate for CNT growth from an Fe catalyst, because alumina is a very good support for Fe as it restricts surface diffusion of Fe and introduces favorable metal-support interactions [36, 38]. Commercially available (McMaster-Carr) thick (area density of 0.9 mg/mm^2) alumina filament cloth woven in a $0^o/90^o$ satin pattern was used. The alumina filaments are ~11 μm in diameter, and each tow

consists of hundreds of filaments, yielding a dry alumina volume fraction of approximately 65 %. The cloth was soaked in a 50 mM solution of $Fe(NO_3)_3 \cdot H_2O$ dissolved in isopropanol for 5 min., and was subsequently dried in ambient air. On the cloth with Fe catalyst, CNTs were grown by our in-house thermal CVD method [35, 38] inside a quartz tube (22 mm ID) furnace at ~750 ^oC. After the temperature is stabilized, hydrogen (H_2) was introduced inside the tube to pre-condition the catalyst on the filament surfaces to form small islands from which the CNTs grow [38, 39-40]. Finally, the carbon source gas, ethylene (C_2H_4), is introduced to start CNT growth, but at a lower flow rate than that for the maximum growth rate. Thus, the growth rate was reduced from ~2 μm/sec to ~0.3 μm/sec for better control of CNT length, so that CNT weight fraction effects on properties could be studied. Three different growth times (0.5, 2, 5 min.) were employed in this research. The CNT length with 5 min. growth time is ~100 μm, which is longer than the spacing between the cloth plies (~10 μm) or the spacing between filaments (~5 μm). The CNTs were observed to grow perpendicular to the filament surfaces as shown in Fig. 1. The CNTs grown using this method were previously characterized by transmission electron microscopy to be multi-walled (~3-5 walls) with a typical outer diameter of ~10 nm. The well-ordered parallel-wall structure observed in TEM indicates the CNTs are of high graphitic quality [38]. The

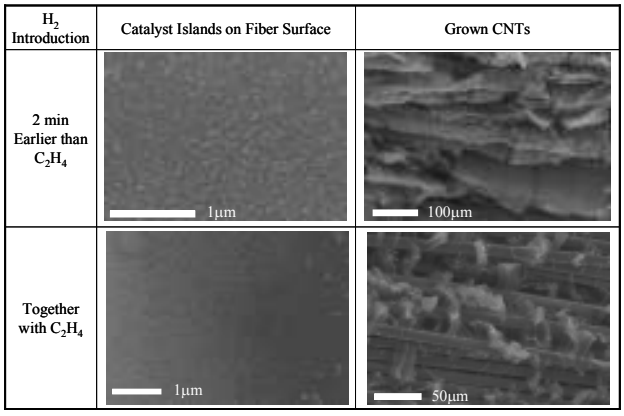

Figure 2. SEM images of the catalyst islands, and CNTs grown on alumina filament surfaces with different H_2 introduction times, illustrating effect of catalyst particles on growth.

conditions for pre-treatment of the catalyst have a large influence on the distribution, density, and the growth speed of the CNTs [38, 39-40]. The catalyst concentration and application method, the sample location inside the tube furnace, and the timing and duration of H_2 introduction were varied to optimize the uniformity and density of CNT growth. For example, the morphology of the catalyst islands, and the CNTs grown on these islands, with different H_2 introduction timings are compared in Fig. 2. The catalyst islands with smaller size (~50-100 nm) and better uniformity showed more dense and uniform CNT growth. For composite sample fabrication, CNTs were grown with the best recipe from the parametric study. Each cloth was weighed using a microbalance (resolution of ~1 μg) before and after the CNT growth to measure the CNT mass grown on the cloth. With 2 min. growth, the CNT mass averaged over 15 samples was 14.8 mg. CNT mass and volume fraction in the final hybrid composite (cloth, polymer, and CNTs) varied from 0.5~2.5 %, and 1~3 %, respectively, while CNT mass and volume fraction in the epoxy varied from 1.7-12 %, and 1.6-10 %, respectively.

2.2 Design and Fabrication of Hybrid Composite Specimens

The sizes of both baseline and hybrid composites were smaller than ~20x40 mm^2 due to limited CNT growth area inside the furnace tube (22 mm ID). The number of the cloth layers varied from 1 to 3, and was kept small to satisfy geometrical requirements (aspect ratio of thickness to shortest in-plane length) imposed by testing standards. As mentioned above, hybrid composites with CNTs of uniformly

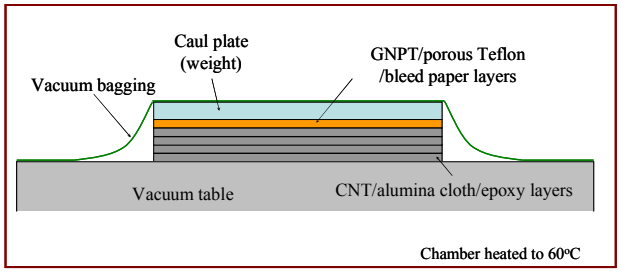

Figure 3. Configuration of alumina filament cloth lay-up during curing process under vacuum (not to scale). (GNPT=guaranteed nonporous Teflon)

different lengths (~30-100 μm) achieved by different growth times (0.5-5 min.) were compared, to the baseline composites without CNTs.

The composites were fabricated by the following procedure. First, alumina cloth coated with CNTs was soaked in epoxy (West Systems 105 Epoxy Resin, 1000 cP at 22 °C) which is curable at room-temperature [41]. The cloth plies were stacked with a weight placed on top, and according to the manufacturer's instructions were cured for 9-12 hours under vacuum with ~200 kPa of pressure (including the weight and the vacuum) at an elevated temperature (~60 ^{o}C) to promote epoxy flow for better wetting and to accelerate the curing time (see Fig. 3). The cured composite specimens were shaped using a band-saw with a fine blade, and the edges were smoothed with sandpaper to form rectangular specimens. Images of the alumina filament cloth (with and without CNTs) and fabricated samples (hybrid and baseline) are shown in Fig. 4.

2.3 Specimen Characterization

The geometry, wetting, and composition of the hybrid composites were characterized. First, the cut edge surfaces of the composites were inspected using an optical and scanning electron microscopy (SEM) to evaluate the wetting of the alumina filaments and CNTs in epoxy. The cut surfaces of the specimens inspected optically and with SEM as in Fig. 5 showed excellent wetting, and the volume of voids was estimated as <~2 % [33] for both specimens with and without CNTs. The dark rings around alumina filaments in the hybrid composites as shown in the lower right image in Fig. 5 is due to SEM charging on the insulating fibers interacting with the conductive epoxy/CNT matrix. Second, the geometries (thickness, width, and length) of the composites were measured with a caliper (resolution of ~2.5x10^{-2} mm). The variation of the length and the width were limited to less than <~ ± 2 %, while the thickness varied by up to ~12 % likely due to non-uniform pressure application during curing process under vacuum. The average ply

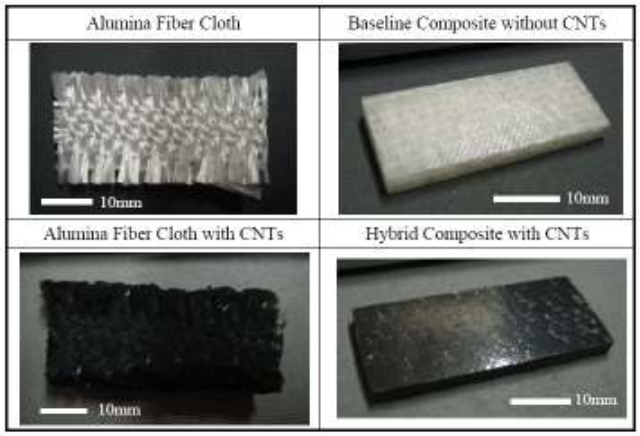

Figure 4. Pictures of the alumina fiber cloths (with and without CNTs), and composites (baseline without CNTs and hybrid with CNTs)

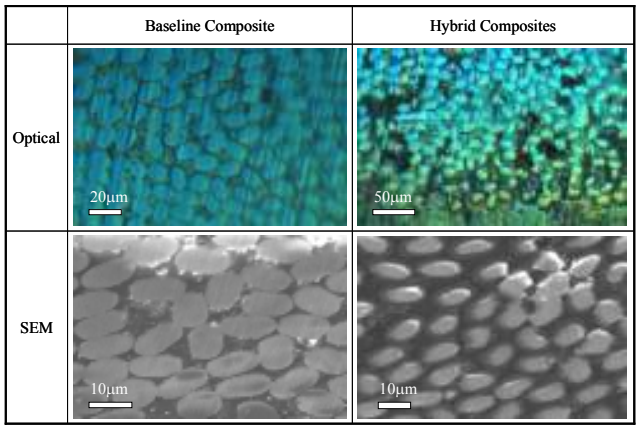

Figure 5. Optical and SEM images of the cut surface cross-sections of baseline (left) and hybrid (right) composites.

thickness for the baseline composites (~0.6 mm) was slightly thinner than that of the hybrid composites (~0.7 mm). Third, mass and volume fractions of CNTs were estimated for each hybrid composite. As mentioned above, each cloth was weighed before and after the CNT growth process, and thus the mass of the cloth coated with catalyst and the grown CNTs were therefore known. Assuming that this measured mass ratio between the CNTs to the alumina cloth with catalyst stays constant during the epoxy curing process, the masses of the alumina filament cloths with catalyst and the CNTs inside composites were estimated by multiplying the ratio of the cut cured sample areas to the original cloth dimension (~20x40 mm^2) respectively with the previously measured masses of the cloth with catalyst and that of the

CNTs. The epoxy mass was estimated by subtracting the mass of the cloth with catalyst and of the CNTs from the measured total composite masses. The CNT weight fractions were calculated based on the mass fraction using the epoxy density of 1.18 mg/mm^3 [41], and the CNT density as 1.4 mg/mm^3 assuming the CNT is a solid cylinder [42-44]. The CNT mass fraction was ~ 0.5-2.5 %, while the CNT volume fraction was estimated as ~1-3 %. Possible catalyst mass reduction from the CVD process and handling were not considered in the CNT mass assessment, leaving this estimate conservative. The CNT fraction in the composites increased with their growth time, as will be discussed below. The volume fraction of alumina filaments in the hybrid composite was ~60 %, and that of epoxy was ~40 %.

3 Intralaminar Composite Multifunctional Testing

The composites were characterized for their electrical resistivity, damping ratio, and Young's modulus. The properties were compared with those of the baseline composites without CNTs to determine property changes introduced by including ~1-3 % volume fractions of aligned radially-grown CNTs on the alumina filament surfaces.

3.1 Volume Electrical Resistivity

The DC electrical resistivities of the samples were experimentally obtained according to the ASTM standards D257-99 for the baseline composites and D4496-04 for the moderately conductive hybrid composites. Volume resistivity was measured in both through-thickness and in-plane directions. Silver paint (SPI Flash Dry Silver Paint) was applied to the relevant surfaces of the composite, which functioned as non-guarded electrodes. The wiring configuration of the test setup was chosen to minimize voltage loss in the circuit, as shown in Fig. 6. The voltage applied to the samples was cycled 5 times between ~0-20 V. The maximum voltage, ~20 V, was kept smaller than the standards specifications (~500 V) to avoid melting and

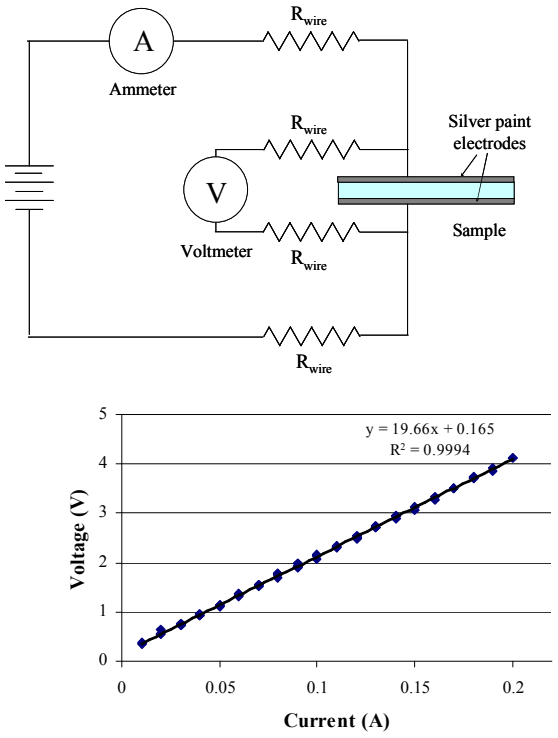

Figure 6. The wiring configuration of the test setup for electrical resistivity measurement in through-thickness direction (top), and the current-voltage slope example of a 2-layer hybrid composite (bottom).

degrading the epoxy due to Joule heating. The measured current-voltage curves were linear (R-squared value > 0.9) as shown in Fig. 6, and the resistance was calculated as the plot slope. The resistivity was calculated based on Eq. 1.

$$\rho_v = R_v \frac{A}{t} \qquad (1)$$

Where A, t, R_v, and ρ_v are area, thickness, resistance, and resistivity.

3.2 Damping Ratio and Young's Modulus

The damping ratios and Young's moduli of the hybrid composites were obtained and compared with those of the baseline composites without CNTs. The rectangular cross-section (thickness: 0.6-2.0 mm, width: 11.4-16.4 mm, length: 30.5-38.5 mm) composites were clamped to a rigid fixture, and were excited by a tip displacement (~3 mm), exciting primarily the cantilever's first mode which is clearly evident in the measured frequency spectra. The vibration velocities at the tip were recorded with

Table 1. Electrical resistivities (in-plane and through-thickness) and damping ratio of baseline and hybrid composites with different number of plies (top, 2 min growth time) and growth time (bottom, 2 plies).

# of plies	Thickness [mm]	In-Plane Resistivity [Ohm mm]		Through-thickness Resistivity [Ohm mm]		Damping Ratio	
		Base	Hybrid	Base	Hybrid	Base	Hybrid
1	~0.6	2.1×10^{8}	9.3 (CNT 1.2 %)	-	69.2 (CNT 1.2 %)	0.0512	0.0476 (CNT 1.2 %)
2	~1.2	7.3×10^{6} 7.8×10^{6}	7.1 (CNT 2.3 %) 9.2 (CNT 2.3 %)	3.1×10^{9} 2.0×10^{9}	82.5 (CNT 2.3 %) - (CNT 2.3 %)	0.0183 0.0327	0.0130 (CNT 2.3 %) 0.0186 (CNT 2.3 %)
3	~1.8	1.3×10^{7}	8.6 (CNT 2.2 %)	2.3×10^{9}	68.2 (CNT 2.2 %)	-	0.0160 (CNT 2.2 %)

Growth Time	CNT Volume Fraction [%]	In-Plane Resistivity [Ohm mm]	Through-thickness Resistivity [Ohm mm]	Damping Ratio
Baseline A	0.0	7.3×10^{6}	3.1×10^{9}	0.0183
Baseline B	0.0	7.8×10^{6}	2.0×10^{9}	0.0327
0.5 min	0.6	131.5	528.6	0.0139
2 min A	2.3	7.1	82.5	0.0130
2 min B	2.3	9.2	-	0.0186
5 min	2.9	9.7	64.6	0.0271

a laser vibrometer (Polytec PSV-300H). Both the samples on the fixture and the laser vibrometer were firmly attached to an air table, isolated from external vibrations. Vibration frequencies were estimated from these averaged signals through FFT (resolution of 153.6 mHz), and were averaged over 5 measurements per sample.

The damping ratio was calculated using the half-bandwidth method [44], as expressed in the following Eq. 2.

$$\varsigma = \frac{f_2 - f_1}{2 f_p} \qquad (2)$$

where f_p is the peak frequency (1st mode natural), and f_1 and f_2 are the frequencies where the signal has the magnitude of $1/\sqrt{2}$ of the peak value at f_p.

The Young's moduli of the samples were also obtained from the same dynamic measurements. If the composites are homogeneous and isotropic along the beam, with a fixed-free boundary condition, the average Young's modulus (E) can be calculated by the following Eq. 3 [45] from small-displacement simple beam theory.

$$\beta_n l = 1.87510407 \qquad (3)$$

with

$$\beta_n^{\,4} = \frac{\rho b h f_n^{\,2}}{EI}, \quad f_n = \frac{1}{\sqrt{1-2\varsigma^2}} f_p$$

$$I = \frac{1}{12} b h^3 \text{ (for rectangular beam).}$$

4 Experimental Results

The property changes made to woven composites by introducing CNTs will be presented in this section. Electrical properties increased with increasing CNT fraction regardless of the number of plies, suggesting good contact between consecutive cloth plies which is attributed to CNTs bridging the matrix-rich interlayer at the ply interfaces.

The damping ratio *decreased* slightly with the addition of CNTs, possibly indicating strong interfaces between the CNTs and the matrix or non-sufficient CNT fractions for a damping effect. Young's modulus data obtained through the vibration tests was inconclusive.

4.1 Electrical Properties

CNT introduction to the alumina filament/epoxy composites significantly decreased the electrical resistivities as summarized in Table 1. The resistivities of

samples with different number of layers or growth time (CNT lengths/fraction) are compared with those of baseline composites. Overall, the composites (both baseline and hybrid) showed higher resistivities in the through-thickness direction, possibly because epoxy blocks electron paths in the through-thickness direction at ply interfaces and at the laminate surfaces. Both the in-plane and through-thickness resistivities significantly decreased, by a factor of 10^6-10^8 with the CNT volume fraction of 1-3 %, regardless of the number of the layers, which is comparable with the past result with CNTs grown on SiC filaments with a different process (10^7 with 2 wt% of CNT) [36]. This both in-plane and through-thickness resistivity improvement demonstrates that a percolation network is effectively formed by CNTs, which would be expected at weight fractions <<1 % as discussed previously with Fig 1. The electrical resistivities of the samples with different CNT mass percentage were also compared in Table 1. Both in-plane and through-thickness resistivities showed decreasing tendency along with the CNT mass percentage. On the other hand, the relative fractions of epoxy or alumina in the composites did not have a significant influence on electrical resistivities.

4.2 Damping Ratio

The damping ratios of the hybrid and baseline composites are also compared in Table 1. No significant correlation was observed between the damping ratio and the CNT mass fraction, although the hybrid composites had on average a *lower* damping ratio by ~31 %. The results were sorted in order of the number of the plies together with CNT volume fraction in Table 2.

We initially expected that introducing CNTs would increase the damping ratio of the composites. Zhou et al. [13] observed an increase in damping with single-walled CNTs in a polycarbonate matrix attributed to CNTs' very large interfacial contact area and frictional sliding/energy dissipation. Thus, size and specific surface area of the CNTs are major factors suggested that affect damping. Damping with increasing single-walled CNT fraction was experimentally observed. Similarly, large damping ratio increase was experimentally observed by other groups [37, 47]. However, this effect was not observed in our results, possibly due to four reasons. First, the CNTs embedded in the composite had large aspect ratio (length to the diameter, L/D). Finegan et al. [48] have theoretically modeled damping in carbon nanofibers/polypropylene matrices, finding that the loss factor decreases with increasing aspect ratio, and suggesting the existence of an optimal aspect ratio for increased damping. Compared with the aspect ratio of the improved cases given above (~700 [47], ~3,000 [37, 49]), the aspect ratio of our CNTs are much larger (~10,000). Second, the amount of CNTs may not have been sufficient enough to alter the damping effects [50]. Third, epoxy/alumina fractions varied slightly from samples to samples, which does not give an ideal comparison between sample with and

Table 2. Damping ratio of baseline and hybrid composites sorted by number of layers

	Volume fraction (%)			
# of plies	CNT	Al2O3	Epoxy	Damping Ratio
1	0.0 (Baseline)	-	-	0.0512
1	1.2 (2 min)	17.5	81.3	0.0476
2	0.0 (Baseline A)	62.2	37.8	0.0183
2	0.0 (Baseline B)	62.4	37.6	0.0327
2	0.6 (0.5 min)	62.7	36.8	0.0139
2	2.3 (2 min A)	62.6	35.2	0.0130
2	2.3 (2 min B)	60.5	37.2	0.0186
2	2.9 (5 min)	48.3	48.8	0.0271
3	2.2 (2 min)	76.3	21.6	0.0160

without CNTs. Filament volume fractions in two samples (2nd and 8th in Table 2) are noted to be far from the average of ~62% due in these cases to issues in the manufacturing of these two specific specimens. However, while the volume fraction for these 2 samples did vary from the average, they are included in the data set as their volume resistivities are in line with the other data. Last, but not least, strong bonding between the CNTs and the matrix may reduce the effect of damping at the CNT surfaces.

We did expect that the Young's modulus would improve somewhat by the short CNTs embedded inside the bulk epoxy and alumina filament composites, in agreement with previous observations [37, 50]. Our results showed a high variation both for the baseline and hybrid composites (~30-300 GPa, C.O.V. of 55 % for baseline composite, and ~140-300 GPa, C.O.V. of 26 % for hybrid composite). Causes for this scatter are likely the large thickness variations observed (discussed previously), epoxy/alumina fraction variation, the imperfect clamping of the cantilever samples in the setup (which changes effective beam length), and inaccuracy of the assumption of isotropic homogeneity for samples having 2-3 layers. Future work will improve manufacturing (specimen geometry) and/or use simple tension to assess composite modulus.

5 Conclusions and Recommendations

Hybrid composites were fabricated by growing CNTs directly on the surfaces of ceramic filament cloth and curing the cloth plies in thermoset epoxy. The electrical and vibration properties were characterized by standard methods and parametrized by varying the number of plies and CNT length within the composites. Incorporation of CNTs imparts electrical conductivity to otherwise insulating composites, which is reflected in a ~10^8 reduction in through-thickness and in-plane electrical resistivities. Resistance is noted to decrease with increased CNT volume fraction in the range of 1-3%. The damping ratio of hybrid CNT-alumina composites is relatively unchanged from the baseline values, and we expect this is due to the high aspect ratio of the aligned CNTs as well as strong CNT-matrix adhesion.

Since the properties of the individual CNTs grown using our process have not yet been characterized, prediction of composite characteristics based on nano- and micromechanical modeling is left for future work. Additional future work includes a wider parametric study of the multifunctional properties as related to CNT geometry (diameter), CNT volume fraction (higher), and engineering of the interfaces (CNT/matrix, matrix/filament, CNT/filament) by directed chemical treatment such as surface functionalization. Additional property characterization will include direct measurement of the elastic modulus, and will be extended to measurement of thermal conductivity and thermal expansion. Finally, this hybrid architecture can be extended to other filament and matrix materials such as carbon filaments, and other structural CNT implementations into traditional composites including nanostitching of prepreg [51], which is of particular interest for aerospace structural applications.

Acknowledgements

This work was supported by Airbus S.A.S and MIT's Karl Chang (1965) Innovation Fund. The authors gratefully thank John Kane, Sunny Wicks, and the entire Technology Laboratory of Advanced Materials and Structures (TELAMS) at MIT for valuable discussions, technical support, and fabrication assistance leading to this work. Sunny Wicks acknowledges undergraduate research opportunity (UROP) support from MIT's Paul E. Gray (1954) Fund.

References

[1] Iijima S. "Helical microtubules of graphitic carbon," *Nature*, Vol. 354, pp. 56-58, 1991.

[2] Treacy M. M. J., Ebbesen T. W., and Gibson T. M. "Exceptionally high young's modulus observed for individual carbon nanotubes." *Nature*, Vol. 381, pp. 680–687, 1996.

[3] Wong E. W., Sheehan P. E., and Lieber C. M. "Nanobeam mechanics: elasticity, strength, and toughness of nanorods and nanotubes." *Science*, Vol. 277, pp. 1971–1975, 1997.

[4] Yu M. F., Files B. S., Arepalli S., and Ruoff R. S. "Tensile loading of ropes of single wall carbon nanotubes and their mechanical properties." *Physical Review Letters*, Vol. 84, No. 24, pp. 5552–5555, 2000.

[5] Yu M. F., Lourie O., Dyer M. J., Moloni K., Kelly T. F., and Ruoff R. S., "Strength and breaking mechanism of multi-walled carbon nanotubes under tensile load." *Science*, Vol. 287, No. 28, 2000.

[6] Ebbesen T. W., Lezec H. J., Hiura H., Bennett J. W., Ghaemi H. F., and Thio T. "Electrical conductivity of individual carbon nanotubes." *Letters to Nature*, Vol. 382, 1996.

[7] Ebbesen T. W. "Carbon nanotubes." *Annual Review of Materials Science*, Vol. 24, pp. 235-264, 1994.

[8] Wildoer J. W. G., Venema L. C., Rinzler A., Smalley R. E., and Dekker C. "Electronic structure of atomically resolved carbon nanotubes." *Nature*, Vol. 391, pp. 59-61, 1998.

[9] Smalley R. E., Dresselhaus M. S., Dresselhaus G., and Avouris P. "*Carbon nanotubes: synthesis, structure, properties and applications*." Springer-Verlag, 2000.

[10] Dresselhaus M. S., Dresselhaus G., and Eklund P. C. "*Science of fullerenes and carbon nanotubes.*" Academic Press, 1996.

[11] Ruoff R. S., and Lorents D. C. "Mechanical and thermal properties of carbon nanotubes." *Carbon*, Vol. 33, No. 7, pp. 925-930, 1995.

[12] Pop E., Mann D., Wang Q., Goodson K., and Dai, H. "Thermal conductance of an individual single-wall carbon nanotube above room temperature." *Nano Letters*, Vol. 6, No. 1, pp. 96 -100, 2006.

[13] Zhou X., Shin E., Wang, K. W., and Bakis C. E., "Interfacial damping characteristics of carbon nanotube-based composites." *Composites Science and Technology*, Vol. 64, pp. 2425-2437, 2004.

[14] Gibson R. F., Ayorinde E. O., and Wen Y. F. "Vibration of carbon nanotubes and their composites: a review." *Composites Science and Technology*, Vol. 67, pp. 1-28, 2007.

[15] Dai H., Hafner J. H., Rinzler A. G., Colbert D. T., and R. E. Smalley. "Nanotubes as nanoprobes in scanning probe microscopy." *Letters to Nature*, Vol. 384, No. 14, pp. 147-150, 1996.

[16] Wong S. S., Joselevich E., Woolley A. T., Cheung C. L., and Lieber C. M. "Covalently functionalized nanotubes as nanometer-sized probes in chemistry and biology." *Letters to Nature*, Vol. 94, 1998.

[17] Yaglioglu O., Martens R., Hart A. J., and Slocum A. H., "Conductive carbon nanotube composite micro-probes." *Advanced Materials* (under review).

[18] Rice P. "Broadband electrical characterization of multiwalled carbon nanotubes and contacts." *Nano Letters* (under review)

[19] Collins P.G., and Avouris P. "Nanotubes for Electronics," *Scientific American*, Vol. 283, Vol. 6, 2000.

[20] Routkevitch D., Tager A. A., Haruyama J., Almawlawi D., Moskovits M., and Xu J. M., "Nonlithographic nano-wire arrays: fabrication, physics, and device applications." *IEEE Transactions on Electron Devices, Special Issue on Future Trends*, Vol. 43, No. 10, pp. 1646-1658, 1996.

[21] Bennett R. D., Hart A. J., and Cohen R. E. "Controlling the morphology of carbon nanotube films by varying the areal density of catalyst nanoparticles using block copolymer micellar thin films." *Advanced Materials*, Vol. 18, pp. 2274–2279, 2006.

[22] Futaba D. N., Hata K., Namai T., Yamada T., Mizuno K., Hayamizu Y., Yumura M., and Iijima S. "Catalyst activity of water-assisted growth of single walled carbon nanotube forest characterization by a statistical and macroscopic approach." *Journal of Physical Chemistry B*, Vol. 110, No. 15, pp. 8035–8038, 2006.

[23] Cantoro M., Hofmann S., Pisana S., Scardaci V., Parvez A., Ducati C., Ferrari A.C., Blackburn A.M., Wang K.-Y., and Robertson J. "Catalytic chemical vapor deposition of singlewall carbon nanotubes at low temperatures." *Nano Letters*, Vol. 6, No. 6, pp. 1107–1112, 2006.

[24] Hata K., Futaba D. N., Mizuno K., Namai T., Yumura M., and Iijima S. "Water-assisted highly efficient synthesis of impurity-free single-walled carbon nanotubes." *Science*, Vol. 306, No. 5700, pp. 1362–1364, 2004.

[25] Hart A. J., and Slocum A. H. "Force output, control of film structure, and microscale shape transfer by carbon nanotube growth under mechanical pressure." *Nano Letters*, Vol. 6, No. 6, pp. 1254–1260, 2006.

[26] Thostenson, E. T., Li, C., and Chou, T. W. "Nanocomposites in context." *Composite Science and. Technology,* Vol. 65, pp. 491–516, 2005.

[27] Calvert P. "Nanotube composites: a recipe for strength." *Nature,* Vol.399, pp. 210–211, 1999.

[28] García E. J., Hart A. J., Wardle B. L., and Slocum A. H. "Fabrication of composite microstructures by capillarity-driven wetting of aligned carbon nanotubes with polymers." *Nanotechnology*, Vol. 18, 2007.

[29] Park C., Wilkinson, J., Banda S., Ounaies, Z., Wise K. E., Sauti G.,Lillehei P. T., and Harrison J. S. " Aligned single-wall carbon nanotube polymer composites using an electric field." *Journal of Polymer Science, Part B: Polymer Physics*, Vol. 44, No. 12, pp. 1751-1762, 2006.

[30] Jin L., Bower C., and Zhou O. "Alignment of carbon nanotubes in a polymer matrix by mechanical stretching." *Applied Physics Letters*, Vol. 73, No 9, pp. 1197-1199, 1998.

[31] Thostenson E. T., Li W. Z., Wang D. Z., Ren Z. F., and Chou T. W. "Carbon nanotubes/carbon fiber hybrid multiscale composites." *Journal of Applied Physics*, Vol. 91, pp. 6034-6037, 2002.

[32] García E. J., Hart A. J., Wardle B. L., and Slocum A. H. "Fabrication and testing of long carbon nanotubes grown on the surface of fibers for hybrid composites." *Proceedings of 47th AIAA/ASME/ASCE/AHS/ASC Structures, Structural Dynamics, and Materials Conference*, Newport, RI, 2006.

[33] García E. J., Hart A. J., Wardle B. L., and Slocum A. H. "Aligned carbon nanotube reinforcement of ply interfaces in woven composites." *Proceedings of 48th AIAA/ASME/ASCE/AHS/ASC Structures, Structural Dynamics, and Materials Conference*, Waikiki, HI, 2007.

[34] Gojny F. H., Wichmann M. H. G., Köpke U., Fiedler B., and Schulte K. "Carbon nanotube-reinforced epoxy-composites: enhanced stiffness and fracture toughness at low nanotube content." *Composites Science and Technology*, Vol. 64, pp. 2363-2371, 2004.

[35] Hart A. J., and Slocum A. H. "Versatility of the Fe/Al_2O_3 System for High-Yield Carbon Nanotube Growth by Thermal CVD of C_2H_4," *Proceedings of 6th International Conference on the Science and Application of Nanotubes*, Göteborg, Sweden, p. 28, 2005.

[36] Hart A. J., and Slocum A. H. "Flow-mediated nucleation and rapid growth of millimeter-scale, aligned, carbon nanotube structures from a thin film catalyst." *Journal of Physical Chemistry B*, Vol. 110, No.16, pp. 8250-8257, 2006.

[37] Veedu V. P., Cao A., Li X., Ma K., Soldano C. S., Kar S., Ajayan P. M., and Ghasemi-Nejhad M. N. "Multifunctional composites using reinforced laminae with carbon-nanotube forests." Nature Materials, Vol. 5, pp. 457-462, 2006.

[38] Hart A.J. "*Chemical, Mechanical, and Thermal Control of Substrate-Bound Carbon Nanotube Growth*." PhD thesis, Department of Mechanical Engineering, Massachusetts Institute of Technology, 2006.

[39] Endo M., Muramatsu H., Hayashi T., Kim Y. A., Terrones M., and Dresselhaus M. S. "'Buckypaper' from coaxial nanotubes." *Nature*, Vol. 433, pp. 476, 2005.

[40] Franklin N. R., and Dai H. J. "An enhanced CVD approach to extensive nanotube networks with directionality." *Advanced Materials*, Vol. 12, No. 12, pp.890–894, 2000.

[41] West Systems Inc. (2006). "Epoxy Product Guide." Retrieved April 30th, 2007, from http://www.westsystem.com/

[42] Krishnan A., Dujardin E., Ebbesen T.W., Yianilos P. N., and Treacy M. M. J. "Young's modulus of single-walled nanotubes." *Physical Review B*, Vol. 58, No. 20, pp. 14013–14019, 1998.

[43] Barber A. H., Andrews R., Schadler L. S., and Wagner H. D. "On the tensile strength distribution of multiwalled carbon nanotubes." *Applied Physics Letters*, Vol. 87, pp. 203106–1–3, 2005.

[44] Kim P., Shi L., Majumdar A., and McEuen P. L. "Thermal transport measurements of individual multiwalled nanotubes." *Physical Review Letters*, Vol. 8721, No. 21, 2001.

[45] Nashif A.D., Jones D.I.G., and Henderson J.P. "*Vibration Damping*." Wiley, 1984.

[46] Inman D.J. "*Engineering Vibration*," Prentice Hall, 2001.

[47] Koratkar N. A., Suhr J., Joshi W., Kane R. S., Schadler L. S., Ajayan P. M., and Bartolucci S. "Characterizing energy dissipation in single-walled carbon nanotube polycarbonate composites." *Applied Physics Letter*, Vol. 87, 063102, 2005.

[48] Finegan I.C., Tibbetts G.G., and Gibson R.F. "Modeling and characterization of damping in carbon nanofiber/polypropylene composites." *Composites Science and Technology*, Vol. 63, No. 11, pp. 1629-1635, 2003.

[49] Andrews, R., Jacques, D., Rao, A.M., Rantell, T., Derbyshire, F., Chen, Y., Chen, J., and Haddon, R.C. "Nanotube composite carbon fibers." Applied Physics Letters, Vol. 75, No. 9, p 1329-1331, 1999.

[50] Rajoria, H. and Jalili, N. "Passive vibration damping enhancement using carbon nanotube-epoxy reinforced composites." *Composites Science and Technology,* Vol. 65, No.14, pp. 2079-2093, 2005.

[51] Garcia E.J., Hart A. J., Wardle B. L., Slocum A. H., Shim D. J., "Aligned carbon nanotube reinforcement of graphite/epoxy ply interfaces," *16th International Conference of Composite Materials*. 2007.